

Studies and characterisations of various activated carbons used for carbon/carbon supercapacitors

J. Gamby^a, P.L. Taberna^a, P. Simon^{a,*}, J.F. Fauvarque^a, M. Chesneau^b

^aLaboratoire d'Electrochimie Industrielle, Conservatoire National des Arts et Métiers, 2 Rue Conté, 75003 Paris, France

^bSociété PICA-France, 15 route Foëcy, 18100 Vierzon, France

Received 07 November 2000; received in revised form 16 January 2001; accepted 29 January 2001

Abstract

Various activated carbons from the PICA Company have been tested in supercapacitor cells in order to compare their performances. The differences measured in terms of specific capacitance and cell resistance are presented. Porosity measurements made on activated carbon powders and electrode allowed a better understanding of the electrochemical behaviour of these activated carbons. In this way, the PICTACTIF SC carbon was found to be an interesting active material for supercapacitors, with a specific capacitance as high as 125 F/g. © 2001 Elsevier Science B.V. All rights reserved.

Keywords: Supercapacitor; Activated carbon; Specific capacitance; Porosity

1. Introduction

Supercapacitors are intermediates systems between electrochemical batteries that can store high energy associated with low power values and dielectric capacitors, which can deliver very high power during few milliseconds [1,2]. Supercapacitors can purchase high specific power (from approximately 0.5–5 kW/kg) during few seconds or more, which leads to specific energy densities ranging from 0.5 to 10 Wh/kg. There are three different types of supercapacitors: (i) carbon/carbon [3,4], (ii) metal oxide [5,6], and (iii) electronically conducting polymers [7,8]. This work is focused on carbon/carbon supercapacitors.

In carbon supercapacitors, the electric charge is stored between a high surface area carbon electrode/electrolyte interface. In these systems, the use of organic electrolytes allows the increase of the working voltage as compared to aqueous electrolyte. The electrode is composed of a current collector in contact with an activated carbon. The current collector has to be electrochemically inactive in the potential window in which the system works. The active material is an activated carbon. Under a powder form, activated carbon is mixed with a binder and sometimes with an electronic

conductor in order to reach good mechanical and electronic properties to the electrode. Activated carbons used in supercapacitors must have different characteristics: (i) a high specific surface area (m^2/g) to ensure high specific capacitance value, (ii) a low resistivity, and (iii) a microtexture well adapted in order to allow good electrolyte accessibility into the inner surface of the electrode.

This paper presents the results obtained with various activated carbons from the PICA Company. Relationships between physical and electrochemical properties have been established to select the best carbon to be used in supercapacitors.

2. Experimental

2.1. Activated carbons

Different carbon powders from the PICA Company were electrochemically tested in this work, namely PICA A, B, C, D, E and PICTACTIF SC. Physical characteristics of these materials were measured in the PICA laboratory and are listed in Table 1. Results obtained with the Norit SX Ultra activated carbon in the same experimental conditions are given for comparison.

Specific surface area and pore size distribution (PSD) measurements were performed using a ASAP 2000 Micromeritic. These values are deduced from the Ar adsorption

* Corresponding author. Tel.: +33-1-40-27-24-23;
fax: +33-1-40-27-26-78.
E-mail address: simon@cnam.fr (P. Simon).

Table 1
Physical characteristics of the different activated carbon powders tested

	Norit	PICA A	PICA B	PICA C	PICA D	PICA E	PICACTIF SC
BET surface (m ² /g)	1200	2315	2100	1500	2100	1500	2315
Resistivity (Ω cm)	3	1.99	0.47	0.72	0.47	0.72	1.99

isotherm at the liquid nitrogen temperature. Resistivity has been measured on packed powders.

2.2. Electrodes

The electrodes were constituted by a nickel foam current collector (110 pores/in.) and the active material. Composition of the active material is 95% of activated carbon and 5% of mixture of binder (carboxymethylcellulose and PTFE). After drying, the active material is laminated on each side of the current collector, to make a 600 μm thick electrode. Electrode processing is detailed elsewhere [9,10]. The amount of activated carbon was kept constant for each electrode. Supercapacitor cells were built by assembling two 4 cm² electrodes. A 50 μm thick polyethylene sheet was used as the separator. Fig. 1a shows a schematic view of the 4 cm² test cell, with the PTFE plates and the stainless steel clamps used to improve the contact inside the cell. The cell

is then immersed in the electrolyte and is placed in an argon-filled sealed box.

2.3. Galvanostatic tests

Galvanostatic cycling of supercapacitor cells was performed using a Biologic VMP potentiostat at constant current density of 10 mA/cm² between 0 and 2 V. Each cell was cycled 1000 times. Resistance of the cell was measured at the beginning of charge and discharge by dividing the ohmic drop by the current, with the time resolution of the Biologic potentiostat (20 ms). Capacitance (F) of the cell was deduced from the slope of the $V(t)$ curves: $C_{\text{cell}} = I / (dV/dt)$. Specific capacitance of the activated carbons was calculated as follows: C_{cell} being the total capacitance of the cell (F), m the amount of activated carbon in one electrode (g), the specific capacitance of the activated carbon C is then $C = 2C_{\text{cell}}/m$.

2.4. Electrochemical impedance spectroscopy

Impedance measurements were carried out with a Schlumberger Electrochemical Interface 1286 coupled with a 1255 Frequency Response Analyser. The frequency range studied varied from 65 kHz to 10 MHz.

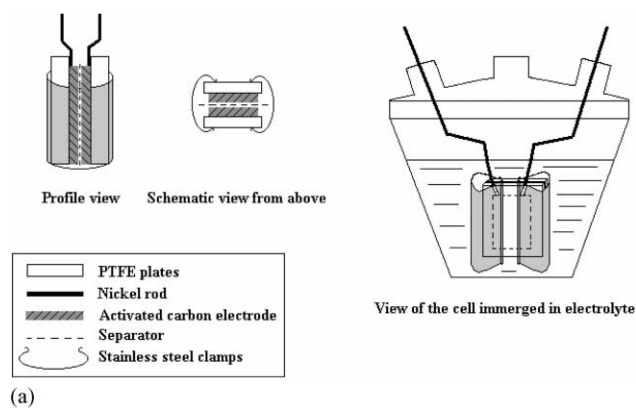
3. Results

3.1. Galvanostatic cycling

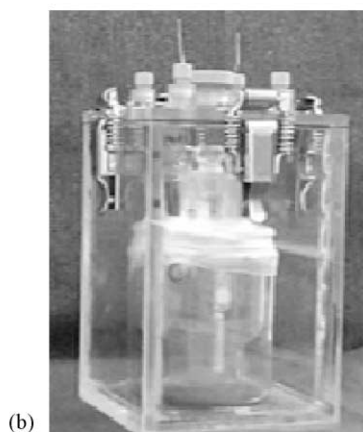
Two-electrode cells of 4 cm² were assembled and galvanostatically cycled at 10 mA/cm² between 0 and 2 V. The electrode composition is as follows: 95% activated carbon and 5% binder (see Section 2).

Two electrolytes were used to perform this study: a solution of $N(C_2H_5)_4CH_3SO_3$ 1.7 M in acetonitrile (TEAMS 1.7 M in AN) and a solution of $N(C_2H_5)_4CH_3SO_3$ 1 M in propylene carbonate (TEAMS 1 M in PC). The conductivity of the AN-based electrolyte is relatively high (25 mS/cm at room temperature), but the low boiling point of AN limits the use of this electrolyte to low temperature (up to 50°C). When PC is used as solvent, the working temperature is greatly increased (up to 100°C and more), but the resistivity of such electrolytes is higher (6 mS/cm at room temperature).

Fig. 2 presents the galvanostatic cycling curve of the cell assembled with the PICA A activated carbon in TEAMS 1.7 M in AN. Resistance and capacitance of the cell were



(a)



(b)

Fig. 1. (a) Schematic view of the 4 cm² test cell; (b) 4 cm² test cell in sealed box to ensure air tightness.

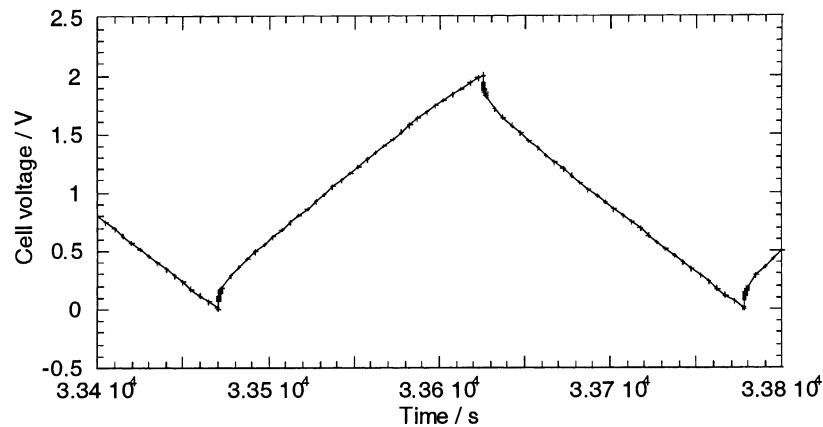


Fig. 2. Galvanostatic cycling curve of the cell assembled with the PICA A-activated carbon in TEAMS 1.7 M in AN.

calculated from this plot. Constant values of the resistance and capacitance were obtained after few cycles. The shape of the cycling curves obtained with the other activated carbons is similar to this one; resistance and specific capacitance were then calculated in the same way for each cell and listed in Table 2.

In the AN-based electrolyte, specific capacitance and resistance of the Norit SX Ultra-based cell were found to be, respectively, 80 F/g and $5 \Omega \text{ cm}^2$, which are the values we previously reported for this carbon [9,10]. Specific capacitance measured for the other carbons is always higher than 80 F/g. It was an expected result, since the specific surface area of this reference product appears to be the lowest. The change of the serial resistance of the cells versus the nature of the activated carbon used is also interesting. It has been mentioned in the literature [11] that an increase of the specific surface area of the carbon generally leads to an increase of the intrinsic resistivity of the material. As can be seen in Table 2, this change seems not to have a measurable effect on the value of the cell's resistance. It appears that the lowest values of the resistance were obtained when the highest surface area carbons (D and PICTACTIF SC) were used as the active materials. The carbon structure also defines the conductivity properties. The latter allows to obtain high value of the specific capacitance (125 F/g)

associated with low serial resistance ($3.5 \Omega \text{ cm}^2$) in AN-based electrolyte.

In carbonate propylene-based electrolyte, the same conclusions can be drawn from Table 2. However, the specific capacitance of the cells is always lower than the one measured in AN, which can be explained by the difference in resistivity and dielectric constant existing between the two solvents [4,12]. The increase of the serial resistance of the cells in the PC-based electrolyte comes from the higher resistance of this electrolyte as compared with AN-based electrolyte.

To summarise this first part of the work, galvanostatic cycling of supercapacitors cells assembled with electrodes containing new activated carbons have shown that high value of specific capacitance (125 F/g) associated with low serial resistance ($3.5 \Omega \text{ cm}^2$) could be obtained when using PICTACTIF SC carbon. These values are largely improved as compared to the one obtained with reference (80 F/g and $5 \Omega \text{ cm}^2$). Porosity measurements must now be carried out in order to understand the difference measured with the various carbons.

3.2. Porosity measurements of activated carbons

Theoretically, when the specific surface area of an activated carbon is increased, so does its specific capacitance. But in fact, the specific capacitance change versus the specific surface is much more complex: the nature and the porosity of the precursor, pore size distribution, the activation treatment and impurities content are some of the most important parameters that govern the ion adsorption process [1,11]. Porosity measurements have then been carried out in order to obtain basic information on the structure of the electrode. Analyses have been made on activated carbon powders and on the electrodes. The electrodes were composed of the active material, obtained by mixing 95% activated carbon and 5% binder (CMC and PTFE), and the nickel foam current collector. Results as a whole are presented in Table 3 and are now going to be detailed.

Table 2
Specific capacitance and series resistance obtained for the two electrodes 4 cm^2 cells assembled with the different activated carbons

Activated carbon	AN/TEAMS		PC/TEAMS	
	Capacitance (F/g)	Resistance ($\Omega \text{ cm}^2$)	Capacitance (F/g)	Resistance ($\Omega \text{ cm}^2$)
Norit	80	5	60	10.5
PICA A	115	6	110	15.5
PICA B	100	6	75	11
PICA C	90	5	70	16
PICA D	105	4	90	11
PICA E	100	5	70	16
PICTACTIF SC	125	3.5	115	10

Table 3

Properties of the different activated carbon powders and electrodes tested, in terms of microporous and mesoporous volume fraction

Electrode	Specific surface area (m ² /g)	Median diameter (Å)	Microporous volume, size < 20 Å (cm ³ /g)	Mesoporous volume, 20 < size < 500 Å (cm ³ /g)	Total porous volume, size < 500 Å (cm ³ /g)
Norit (electrode)	920	14.6	0.34	0.23	0.57
A (powder)	2315	22.1	0.77	0.86	1.63
A (electrode)	1937	24.2	0.70	0.87	1.57
B (powder)	2094	13.9	0.74	0.38	1.12
B (electrode)	1960	19.6	0.65	0.44	1.09
C (powder)	1498	9.3	0.55	0.16	0.71
C (electrode)	1170	10.8	0.43	0.16	0.59
D (electrode)	2088	15.1	0.69	0.40	1.09
E (electrode)	1079	12.0	0.40	0.19	0.59
PICACTIF SC (electrode)	1890	23.4	0.60	0.72	1.32

3.2.1. Specific surface

The change in the microporous volume depending on the specific surface area is presented in Fig. 3. The microporous volume, as defined in Table 3, includes pores with a diameter lower than 20 Å. The linear shape of the plot clearly indicates that the increase of the microporous volume is linked to an increase of the surface area, which was an expected result.

3.2.2. Specific capacitance

Fig. 4 shows the dependence of the BET surface on the specific capacitance of the activated carbons. Surface areas presented in Table 3 were obtained by the BET method. This surface corresponds to the area accessible for gas adsorption. In carbon supercapacitors, the specific capacitance of the carbon is related to its capability to adsorb ions from the electrolyte. This explains why the specific capacitance is not

linearly dependent on the BET surface. It is then clear that the only knowledge of the BET surface of the activated carbons is not sufficient to predict their ionic adsorption efficiency.

Fig. 5 schematically presents the fraction of the activated carbon BET surface that is really accessible to the electrolyte. This representation is derived from the work of Nui et al. [13]: if one considers a mean value of 20 μF/cm² for the double-layer capacitance and if the activated carbon BET surface is 1000 m²/g, then the maximum specific capacitance the carbon could reach would be 200 F/g. This model allows to compare the different activated carbons tested. From the experimental specific capacitances measured for the different carbons, one has calculated the real part of the surface that contributes to the specific capacitance. As an example, the BET surface of the electrode composed of Norit SX Ultra activated carbon is 920 m²/g. Considering

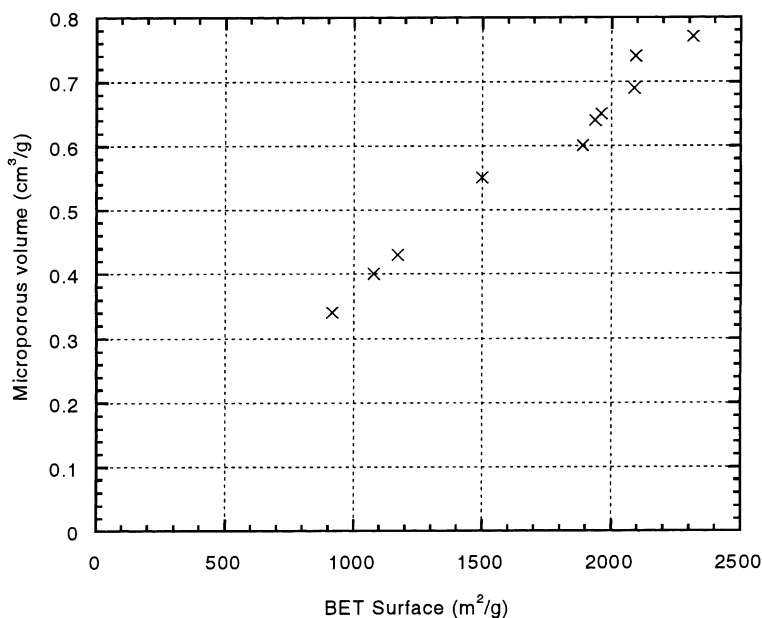


Fig. 3. Microporous volume (pore diameter < 20 Å) vs. BET surface area of the activated carbon powders and electrodes.

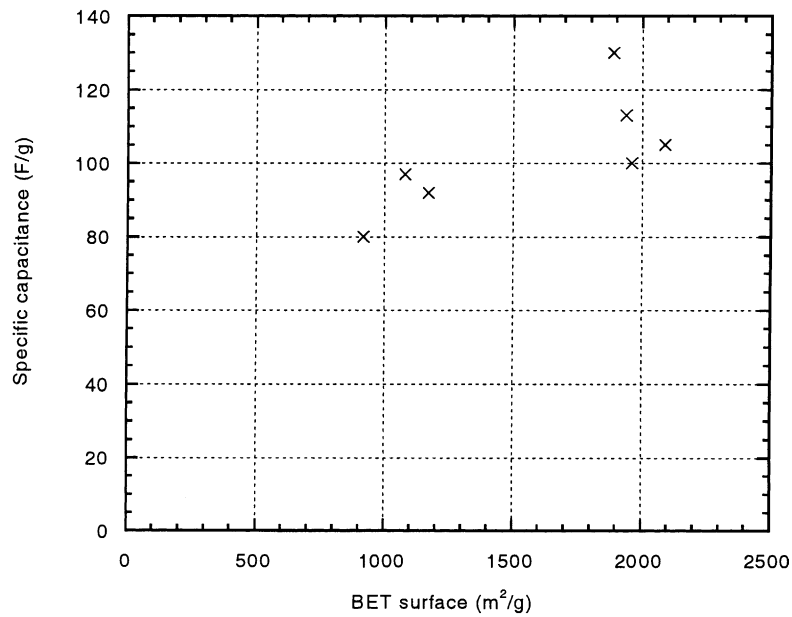


Fig. 4. Specific capacitance vs. BET surface area of activated carbon used for the electrodes.

the mean value of $20 \mu\text{F}/\text{cm}^2$ for the double-layer capacitance, the specific capacitance of this carbon could theoretically reach 182 F/g . In fact, a value of 80 F/g was measured, that means that only 44% of the total BET surface contributes to the specific capacitance. For the highly activated carbons, i.e. for the highest values of the BET surface, there is a significant fraction of electrolyte inaccessible surface due to small pore dimensions. It is then clearly impossible to characterise an activated carbon on the only

basis of its BET surface: the electrolyte pore accessibility has to be taken into account, that is to say the pore size distribution. Indeed, if the increase of the microporous volume leads to an increase of the BET surface, it is clear that the whole part of this microporous volume (pore diameter lower than 20 \AA) would not be accessible to the ions: their size limits their adsorption to the largest pores. There is then a balance to find for the activated carbon between high BET surface and pore size distribution.

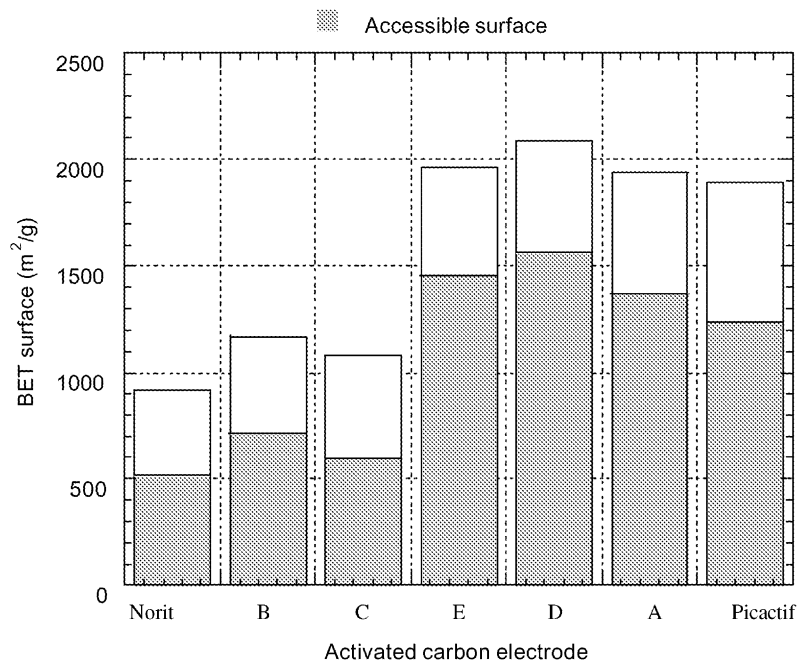


Fig. 5. Specific capacitance of the different activated carbons used for the electrodes: fraction of the electrode surface really accessible to the electrolyte (from [13]).

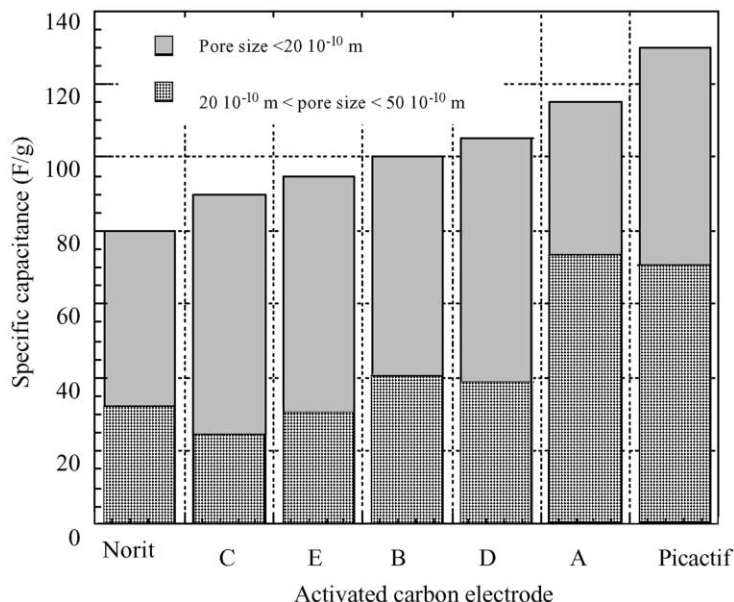


Fig. 6. Specific capacitance of the different activated carbons used for the electrodes: fraction of micro- and mesopores in the electrodes (from data presented in Table 3).

Fig. 6 shows, for each activated carbon, the part of the specific capacitance related to the micropores and the mesopores. This Fig. 6 is based on the data presented in Table 3. It shows, for each of the seven carbons, the dependence of the specific capacitance measured during galvanostatic cycling of the supercapacitors cells on the micro- and mesoporous volume. For example, the Norit-based electrode exhibits a capacitance of 80 F/g with a total porous volume of $0.57 \text{ cm}^3/\text{g}$, divided into $0.23 \text{ cm}^3/\text{g}$ of mesopores (i.e. 41%) and $0.34 \text{ cm}^3/\text{g}$ of micropores (59%). For the high surface area carbons B, C, D and E, the pore volume is composed of micropores in a greater extent. This can explain the comparatively low values of the specific capacitance obtained: the electrolyte pore accessibility is more difficult, leading to the decrease of the surface area used for the adsorption. On the contrary, Norit- and carbon A-based electrodes exhibit higher $\text{Vol}_{\text{mesoporous}}/\text{Vol}_{\text{microporous}}$ ratio. A more important part of the surface can then be used for ion adsorption. It was an expected result for the Norit-based electrode, as its low BET surface guaranteed a lower microporous volume. But in the case of highly activated carbons A and PICTACTIF SC, the situation is different: they associate high surface area (close to $2300 \text{ m}^2/\text{g}$) with a low microporous volume, leading to a capacitance of 125 F/g for the PICTACTIF SC carbon in TEAMS 1.7 M in AN.

From these measurements, PICTACTIF SC carbon appears to be interesting material for applications in the carbon supercapacitors field. Electrochemical impedance measurements have then been carried out on supercapacitors cells in order to characterise their response under a large range of frequency.

3.3. Electrochemical impedance spectroscopy measurements

Fig. 7a and b (enhancement of the high frequency range) present the Nyquist plots for 4 cm^2 cells assembled with two electrodes containing carbons A, B, C and Norit. The frequency range studied is 65 kHz–10 MHz. The voltage between the two electrodes is kept constant at 0 V during the measurements.

At very high frequencies (close to 60 kHz), the imaginary part of the impedance tends to 0 and the resistance measured is composed of several terms: the ionic resistance of the electrolyte, the intrinsic resistance of the active material, and the contact resistance at the interface active material/current collector (the resistivity of the metallic current collector can be here neglected). This explains why the very high frequency resistance of the cells is roughly the same, although the intrinsic resistance of the carbons is different.

At high frequencies, Fig. 7b shows the presence of a loop. This loop has been described elsewhere as a pseudo-transfer resistance [14] and is associated with the porous structure of the electrode. This loop shifts the appearance of the capacitive behaviour (the sharp increase of the imaginary part) towards the high values of the resistance. The amplitude of the loop changes with the nature of the carbon: it is smaller for carbon A and Norit, and increases with carbons B and C. The porosity study has previously shown that the microporous volume was the larger for these two electrodes, leading to a decrease of the ions adsorption efficiency. This difference in the pore size distribution may also explain the difference observed in the impedance behaviour: the

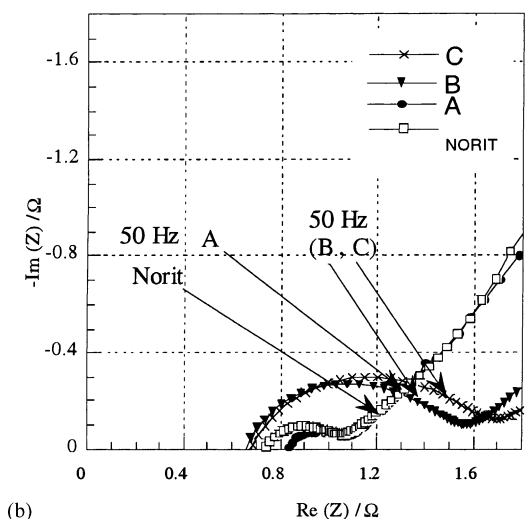
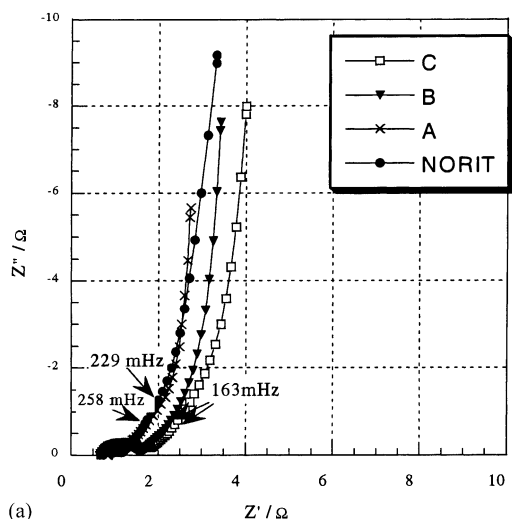


Fig. 7. Nyquist plots for 4 cm² cells assembled with two electrodes containing carbons A, B, C and Norit (a) and high frequency range enhancement (b). Frequency range studied: 65 kHz–10 MHz.

mesoporous structure of the electrode containing carbon A and Norit increases the pore accessibility. The real part of the impedance is then less frequency dependent, and the capacitive behaviour (the sharp increase of the imaginary part) appears at lower resistance values.

At low frequencies, the imaginary part of the impedance sharply increases: this is the capacitive behaviour of the electrode. The total value of the capacitance is reached. The impedance plot should theoretically be a vertical line, parallel to the imaginary axis: $Z = -1/jC\omega$. In fact, a difference between this theoretical behaviour and the experimental one can be observed. Song et al. [15] have recently proposed a new mathematical model to describe this frequency dispersion, taking into account the penetrability coefficient α_0 . The penetration depth of the ac signal inside the porous matrix decreases with the frequency. This means that a porous electrode composed of pores with equal

dimensions presents an impedance that approaches the ideal capacitive behaviour at low frequencies (the vertical line) shifted along the abscissa. If the dimensions of the pores are different, leading to a pore size distribution inside the porous matrix, the penetration of the ac signal is different at the same frequency: the electrolyte accessibility becomes easier for the larger pores, while the ions will not enter into the smallest pores. This leads to a frequency dispersion, as can be seen in Fig. 7, where the low frequency impedance behaviour is shifted from the theoretical vertical line.

These electrochemical impedance spectroscopy measurements have shown interesting properties for carbon A- and Norit-based electrodes: lower resistance associated with better electrolyte pore accessibility. However, on the basis of specific capacitance (115 F/g for carbon A as compared to 80 F/g for Norit), the activated carbon A seems to be a promising active material for carbon supercapacitors.

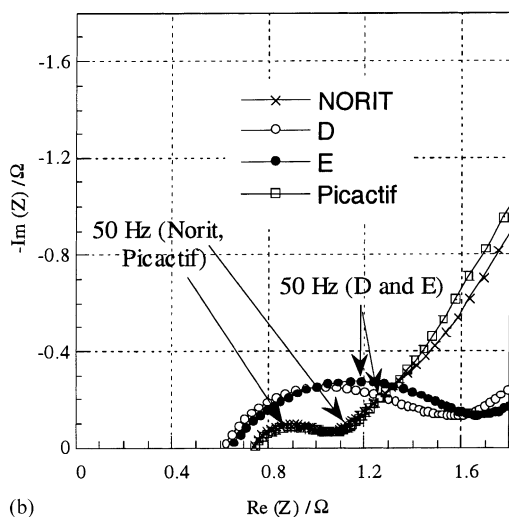
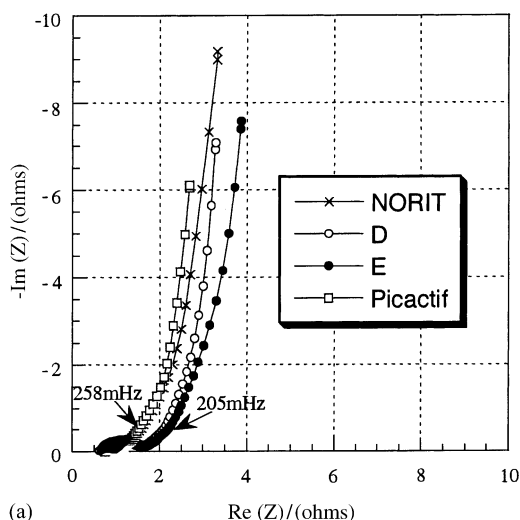


Fig. 8. Nyquist plots for 4 cm² cells assembled with two electrodes containing carbons D, E, PICTACTIF and Norit (a) and high frequency range enhancement (b). Frequency range studied: 65 kHz–10 MHz.

The same measurements were performed on carbons D, E and PICTACTIF SC. The electrodes were made in the same way as previously shown. Fig. 8a and b (enhancement of the high frequency range) presents the Nyquist plot for the 4 cm² cells assembled with electrodes containing carbons D, E, PICTACTIF SC and Norit. The same conclusions can be drawn from these figures: the high frequency loop can be seen in all the impedance diagrams. The amplitude of this loop is more important for carbons D and E as compared to the Norit and PICTACTIF SC carbons. The difference in the porous structure of the electrodes can explain this result: the higher mesoporous volume of the electrodes containing carbons PICTACTIF SC and Norit facilitates the electrolyte accessibility in these larger pores. The real part of the impedance becomes less frequency dependent and the capacitive behaviour appears at lower resistance.

This impedance spectroscopy study confirms the results obtained by galvanostatic cycling. The activated carbon PICTACTIF SC seems to be a suitable material for supercapacitor applications, with a specific capacitance of 125 F/g in AN-based electrolyte. Its porous structure allows a good electrolyte penetration inside the electrode, decreasing the frequency dependence of the real part of the impedance.

4. Conclusions

Activated carbons used as active material in supercapacitors must develop high specific capacitance, associated with low resistivity. These characteristics depend mainly on the nature of the carbon, the BET surface and the porous structure. In this paper, several activated carbons from PICA Company were tested and electrochemically characterised. Galvanostatic cycling of supercapacitor cells have first shown important differences between the activated carbons tested. PICTACTIF SC carbon was found to be particularly interesting, with a specific capacitance of 125 F/g and a series cell resistance of 3.5 Ω cm² in TEAMS 1.7 M in AN. Porosity measurements have then shown that this interesting behaviour could be explained by an increase of the mesoporous volume of the carbon that was thought to facilitate ions accessibility and adsorption on the carbon surface. Electrochemical spectroscopy impedance measurements tend to confirm this hypothesis, showing the decrease of the frequency dependence of the real part of the impedance.

PICTACTIF SC carbon then seems to be a suitable active material for supercapacitor applications.

Future work will be focused on different points: stability of the 4 cm² cell performances during long-time cycling (over 10,000 cycles), characterisation of the self-discharge of the cells, and finally assembling and testing of larger dimension prototypes.

References

- [1] R. Kötz, M. Carlen, *Electrochim. Acta* 45 (2000) 2483.
- [2] B.E. Conway, *Electrochemical Capacitors*, Plenum Press, New York, 1999.
- [3] C.J. Farahmandi, R. Spee, in: *Proceedings of the 8th International Seminar on Double Layer Capacitors and Similar Energy Storage Devices*, Florida Educational Seminar, December 1998.
- [4] T. Morimoto, K. Hiratsuka, Y. Sanada, K. Kurihara, *J. Power Sources* 60 (1996) 239.
- [5] J.P. Zheng, P.J. Cygan, T.R. Jow, *J. Electrochem. Soc.* 142 (1995) 2699.
- [6] P. Kurzweil, O. Schmid, A. Löffler, in: *Proceedings of the 7th International Seminar on Double Layer Capacitors and Similar Energy Storage Devices*, Florida Educational Seminar, December 1997.
- [7] J.P. Ferraris, I.D. Brotherston, D.C. Loveday, in: *Proceedings of the 38th Power Sources Conference*, Cherry Hill, NJ, USA, 8–11 June 1998.
- [8] C. Arbizzani, M. Mastragostino, F. Soavi, *Electrochim. Acta* 45 (2000) 2273.
- [9] L. Bonnefoi, P. Simon, J.F. Fauvarque, C. Sarrasin, J.F. Sarrau, A. Dugast, *J. Power Sources* 80 (1999) 149.
- [10] L. Bonnefoi, P. Simon, J.F. Fauvarque, C. Sarrasin, J.F. Sarrau, P. Lailier, *J. Power Sources* 83 (1999) 162.
- [11] A.G. Pandolfo, A.M. Vasallo, G.L. Paul, in: *Proceedings of the 7th International Seminar on Double Layer Capacitors and Similar Energy Storage Devices*, Florida Educational Seminar, December 1997.
- [12] B.E. Conway, in: *Proceedings of the 3rd International Seminar on Double Layer Capacitors and Similar Energy Storage Devices*, Florida Educational Seminar, December 1993.
- [13] C. Nui, E.K. Sichel, R. Hoch, D. Moy, H. Tennent, in: *Proceedings of the 6th International Seminar on Double Layer Capacitors and Similar Energy Storage Devices*, Florida Educational Seminar, December 1996.
- [14] X. Andrieu, G. Crépy, L. Josset, in: *Proceedings of the 3rd International Seminar on Double Layer Capacitors and Similar Energy Storage Devices*, Florida Educational Seminar, December 1993.
- [15] H.K. Song, H.Y. Hwang, K.H. Lee, L.H. Dao, *Electrochim. Acta* 45 (2000) 2241.